

CHROM. 21 231

## GRADIENT FLOW PROGRAMMING: A COUPLING OF GRADIENT ELUTION AND FLOW PROGRAMMING

VIESTURS LESINS\* and ELI RUCKENSTEIN\*

*Department of Chemical Engineering, State University of New York at Buffalo, Buffalo, NY 14260 (U.S.A.)*

(First received August 30th, 1988; revised manuscript received December 21st, 1988)

---

### SUMMARY

The coupling of flow programming and gradient elution is proposed as an integrated approach to the general elution problem. A model is developed to describe the process in which the flow-rate and mobile phase composition change with time. Experimental results with two model proteins compare favorably with theoretical calculations. A parametric study, experimental and numerical, illustrates the effect of various characteristic parameters. Since initial flow-rates are low, improved front-end resolution can be expected due to an increase in column efficiency. Since the mobile phase composition also changes with time, a wide range of elution strengths can also be applied to the column. This allows for the elution of species which initially are strongly retained.

---

### INTRODUCTION

Even with the judicious selection of operating conditions, the separation of multicomponent mixtures by liquid chromatography (LC) under normal elution is often beset with problems. In many cases, the difficulty is due to the large differences in the relative migration rates of the individual components resulting in what is referred to as the general elution problem. Current methods of attacking the general elution problem include<sup>1-4</sup>: (i) solvent programming; (ii) flow programming; (iii) temperature programming; and (iv) coupled-column operation. In each of these techniques conditions are varied during the separation such that the retention of later eluting bands is reduced as a function of time after sample injection, so that the resolution and widths of early- and late-eluting bands are made more similar.

Few examples have been reported of the combination of two or more of the above individual procedures into a single technique. The purpose of this paper is to explore the feasibility of gradient flow programming (GFP). In this technique gradient elution is coupled with flow programming to yield a new attack on the general elution problem. A mathematical model is developed to describe the procedure. In addition,

---

\* Present address: Occidental Chemical Corporation, Development Center, Buffalo Avenue and 53rd St., Niagara Falls, NY 14303, U.S.A.

a parametric study, both numerical as well as experimental, with two model proteins illustrates the effects of various parameters. Although the present application is restricted to ion-exchange chromatography, GFP can also be applied to other methods.

## THEORY

Before considering GFP, it is useful to briefly review its pure constituents, namely, gradient elution and flow programming. For more comprehensive accounts, the interested reader is referred elsewhere<sup>2-4</sup>.

Gradient elution is performed by varying the composition of the mobile phase with time so as to provide a continual increase in the solvent strength of the mobile phase entering the column. Thus the initial bands from a normal elution procedure have their migration rates decreased and are separated under more optimal conditions. In addition, since solvent strength increases with time, the final bands from a normal elution procedure have their relative migration rates increased to values near the optimum range. In this manner, all bands migrate through the column with near optimum capacity factor values of about 2-5.

Flow programming is a technique where the flow-rate increases as a function of time. A significant increase in front-end resolution (*i.e.*, the earlier eluting species) from flow programming can be achieved relative to normal elution, due to an increase in column efficiency (*i.e.*, plate number). Although column efficiency is reduced for later eluting components, resolution of these bands is often not a problem.

Although solvent programming is probably the best single method in dealing with the general elution problem, it too can suffer from poor front-end resolution. For example, it may not be possible to obtain mobile-phase conditions so as to significantly increase the retention of early-eluting components. This situation could arise with water as the initial solvent in reversed-phase chromatography or with a plain buffered solution (*i.e.*, no additional electrolyte) in ion-exchange chromatography. In these cases, a decrease in the elution strength of the initial solvent is not possible. In addition, changing to another LC method may not always be practical or feasible for the separation at hand. Thus, to improve resolution of these early eluting species, the column plate number must be increased. In other situations, where the capacity factors between the first and last eluting species differ significantly, front-end resolution may once again suffer if the gradient is too steep. In this case, a compromise must be made between analysis time and resolution. Thus, the coupling of gradient elution with flow programming can be useful in many situations. To understand how this occurs, consider the well-known equation for resolution,  $R_s$ , under normal elution conditions<sup>2</sup>:

$$R_s = \underset{\text{I}}{\frac{1}{4}} \left( \underset{\text{II}}{\sqrt{N_2}} \right) \left( \frac{\alpha - 1}{\alpha} \right) \left( \underset{\text{III}}{\frac{k'_2}{1 + k'_2}} \right) \quad (1)$$

where the separation factor  $\alpha = k'_2/k'_1$ , the capacity factor  $k' = (V_R - V_m)/V_m$ , subscripts 1 and 2 refer to components 1 and 2,  $N$  is the plate number,  $V_R$  is the retention volume of the species, and  $V_m$  is the void volume.

The three factors (I, II, III) of eqn. 1 describe the contribution of three different effects to resolution which are essentially independent<sup>2</sup>. Consequently, to control resolution, the three factors of eqn. 1 can be adjusted more or less separately. Separation efficiency as measured by  $N$  (factor I) is varied by changing column length  $L$  or solvent velocity. Column efficiency is increased by increasing column length or by decreasing the flow-rate of the mobile phase, which is the characteristic operating feature of flow programming. The column capacity (factor III) as measured by  $k'$  is varied by changing solvent strength, which is the characteristic operating feature of gradient elution. Thus by combining flow programming with gradient elution, one has complete control of the factors involved in resolution as compared to the partial control offered by flow programming (term I) or gradient elution (term III) used alone, on a given column (term II). Hence improved separations can be expected.

In many cases, mobile phase programming is selected through trial and error. However, it would be advantageous to determine elution programming conditions for a given separation *a priori* from a limited knowledge of the properties of the chromatographic system and the components to be separated. Consequently, it is necessary to understand the influence of mobile phase programming on important retention characteristics such as retention volume, bandwidths, and the resolution of sample compounds. This paper quantitatively considers the dependence of the retention volume on various characteristic operating parameters involved in GFP and compares them to experimental results. The effects of operating conditions on bandwidths and resolution are illustrated experimentally and discussed qualitatively.

A schematic illustration of a GFP apparatus is illustrated in Fig. 1. Pump A delivers a chromatographically weak solvent at a constant flow-rate. Pump B delivers a strong solvent, at a flow-rate which increases with time. These solvents are mixed and sent to the column where separation occurs. Retention in ion-exchange chromatography with GFP will now be described. However, GFP has general applicability to any LC technique in which gradients in solvent strength are employed.

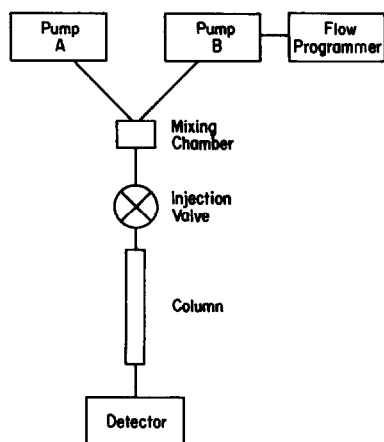


Fig. 1. A schematic illustration of a possible GFP system. In this particular situation, pump A delivers solvent at a constant flow-rate. The flow-rate of the solvent with high elution power increases with time and is delivered by pump B. These solvents are mixed and sent to the column.

## MATHEMATICAL MODEL

*Volumetric flow-rate*

In GFP, the flow-rate and composition are both functions of time. In the present treatment, two solvent-delivery systems are employed to deliver solvent to the column. The flow-rate  $F_A$  of the weak solvent is taken as constant:

$$F_A = a = \text{constant} \quad (2)$$

The flow-rate  $F_B$  of the strong solvent is assumed to increase linearly with time. In the present situation, we assume that the flow-rate is initially zero and increases linearly with time as

$$F_B = bt \quad t < t_G \quad (3a)$$

$$F_B = bt_G \quad t \geq t_G \quad (3b)$$

where  $b$  is a constant,  $t$  is time and  $t_G$  is the total gradient time ( $b$  could also be a function of time). Also note that  $b$  and  $t_G$  may be limited by the maximum allowable column pressure. The significance of  $b$  and  $t_G$  will be discussed later. However, as with gradient elution, times greater than  $t_G$  are not advantageous since elution then essentially becomes isocratic in nature. The total flow-rate  $F$  to the column is simply

$$F = F_A + F_B = a + bt \quad t < t_G \quad (4a)$$

$$F = a + bt_G \quad t \geq t_G \quad (4b)$$

*Gradient composition*

As a specific example, consider ion-exchange chromatography. Let the salt concentrations originating from pumps A and B be denoted by  $x_A$  and  $x_B$ , respectively. The mobile phase concentration  $x$  at the column inlet is therefore given by

$$x = \frac{F_A x_A + F_B x_B}{F_A + F_B} \quad (5)$$

or, by substituting eqns. 2-4 into eqn. 5:

$$x = \frac{ax_A + bx_B t}{a + bt} \quad t < t_G \quad (6a)$$

$$x_G = \frac{ax_A + bx_B t_G}{a + bt_G} \quad t \geq t_G \quad (6b)$$

*Isocratic retention model*

Protein retention in ion-exchange chromatography can be represented by an equation of the form<sup>5,6</sup>

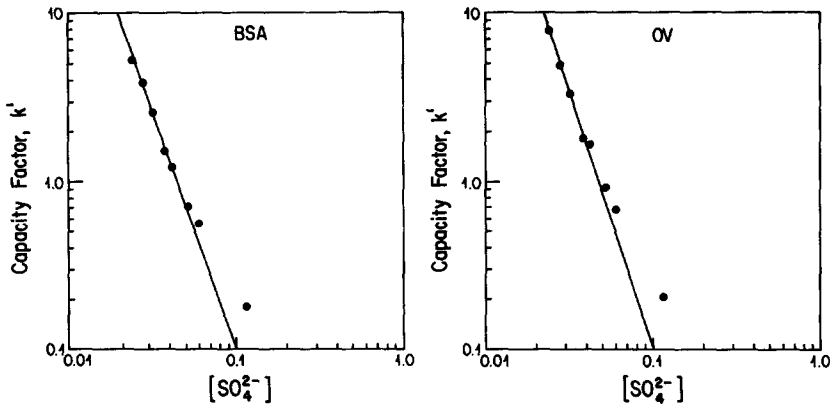


Fig. 2. Isocratic retention data plotted for BSA and OV according to eqn. 7. Isocratic retention parameters derived from linear regression of the data are given in Table I.

$$k' = Kx^m \quad (7)$$

where  $x$  is the salt concentration of the mobile phase,  $K$  is the equilibrium distribution constant for the ion-exchange process and  $m$  is the effective number of charges on the protein which interact with the adsorbent. The parameters  $m$  and  $K$  are evaluated from the slope and intercept of a plot of  $\log k'$  versus  $\log x$ , determined under isocratic conditions. The relationship of the capacity factor to the concentration of the displacing ion for bovine serum albumin (BSA) and ovalbumin (OV) is illustrated in Fig. 2.

Linear regression parameters characterizing the isocratic retention parameters of OV and BSA are summarized in Table I. These isocratic retention parameters are necessary for predicting elution in GFP.

#### Relation of isocratic retention to GFP conditions

The fundamental relationship for gradient elution is given by<sup>3,4</sup>:

$$\int_0^{V_e} \frac{dV}{V_a} = 1 \quad (8)$$

TABLE I

LINEAR REGRESSION PARAMETERS CHARACTERIZING THE ISOCRATIC RETENTION OF BSA AND OV

The error estimates represent the 90% confidence interval.

Protein	$m$	$\log K$	Correlation coefficient
Bovine serum albumin	$-2.83 \pm 0.17$	$-3.83 \pm 0.26$	0.997
Ovalbumin	$-3.04 \pm 0.21$	$-4.02 \pm 0.26$	0.996

where  $V$  is defined by eqn. 10,  $V_g$  is the corrected retention volume ( $V_g = V_R - V_m$ ) of the band at elution at its peak maximum, and  $V_m$  is the column void volume. The instantaneous value of the corrected retention volume at any given time is represented by  $V_a$ , which can be written as

$$V_a = V_m k_a \quad (9)$$

where  $k_a$  is the instantaneous value of  $k'$  for the band.

Substitution of eqns. 5 and 9 into eqn. 8 with

$$dV = Fdt = (a + bt)dt \quad (10)$$

allows eqn. 8 to be rewritten as

$$\int_0^{t_g} \frac{(a + bt)^{m+1}}{(ax_A + bx_B t)^m} dt = KV_m \quad (11)$$

where the time  $t_g$  corresponds to the corrected retention volume  $V_g$ . At this point it is desirable to define the following dimensionless groups:

$$\tau = \frac{at}{V_m} \quad (12)$$

$$\theta = \frac{x_B}{x_A} \quad (13)$$

$$\kappa = \frac{bV_m}{a^2} \quad (14)$$

Note that  $\tau$  is the dimensionless time (which compares the time with the void volume residence time at the initial flow-rate), while  $\kappa$  compares the flow-rate of the strong solvent (at a time equal to the residence time of the weak solvent) with the flow-rate of the weak solvent.

Introducing of eqns. 12–14 into eqn. 11 yields

$$\int_0^{\tau_g} \frac{(1 + \kappa\tau)^{m+1}}{(1 + \theta\kappa\tau)^m} d\tau = Kx_A^m \quad (15)$$

where  $\tau_g$  is the dimensionless retention time corresponding to  $t_g$ . Note that the right-hand side of eqn. 15 is simply the capacity factor which would occur with mobile phase A, in other words, the initial capacity factor. To study the effects of  $\theta$  and  $\kappa$ , which are the fundamental parameters of GFP, a parametric study of these variables was undertaken both numerically as well as experimentally.

## MATERIALS AND METHODS

The essential features of the experimental apparatus are shown in Fig. 1. Two Waters Assoc. (Milford, MA, U.S.A.) Model 6000A solvent delivery systems were employed. Pump B was interfaced with a Waters Assoc. Model 660 solvent programmer. A Rheodyne (Cotati, CA, U.S.A.) Model 7125 injection valve with a 20- $\mu$ l injection loop was employed to load protein onto a Rainin Instruments (Woburn, MA, U.S.A.) Hydropore 300A AX anion-exchange column (25 cm  $\times$  4.6 mm I.D.). Detection was at 280 nm with a Waters Assoc. Model 440 absorbance detector.

Proteins were purchased from Sigma (St. Louis, MO, U.S.A.) and were used without further purification. Other reagents were analytical-reagent grade or of comparable quality. Mobile phases were daily prepared freshly using freshly distilled water from an all-glass still and were passed through a 0.45- $\mu$ m filter. Eluents were prepared by titrating a 0.0025 M sulfuric acid solution with any additional electrolyte required (ammonium sulfate) with imidazole to pH = 7.00  $\pm$  0.02. Initial and final flow-rates were determined by collecting the column effluent in a buret and timed with a stopwatch. It was assumed that the flow-rate of pump B increased linearly with time. The gradient time,  $t_G$ , was monitored with a stopwatch.

## RESULTS AND DISCUSSION

*The effect of solvent strength ratio  $\theta$* 

Before examining experimental and theoretical results illustrating the effect of  $\theta$ , it is worthwhile examining the significance of  $\theta$  and its relation to the separation process. As given by eqn. 13,  $\theta$  is simply the ratio of salt concentrations in the solvent B reservoir and the solvent A reservoir; thus,  $\theta$  is a measure of the increase in solvent strength that can be expected. However, in contrast to most gradient elution procedures which vary linearly from pure A to pure B, this situation does not occur in GFP. As shown by eqn. 6, the composition function can be rewritten in terms of the dimensionless variables as

$$x = x_A \frac{1 + \theta \kappa \tau}{1 + \kappa \tau} \quad \tau < \tau_G \quad (16)$$

Thus, the final composition depends upon the initial concentration  $x_A$ ,  $\theta$ ,  $\kappa$ , and  $\tau_G$  (i.e., the dimensionless time corresponding to  $t_G$ ) and is not  $x_B$  as is the general case for most gradient elution procedures.

Although the only absolute requirement on the nature of solvents A and B is that B be chromatographically stronger than A (and that the two be miscible), several other features deserve comment. For example, as the strength of solvent B is decreased, the elution of later bands becomes slower, and the bands become wider and less easily detectable. Furthermore, bands may elute after the end of the elution program. In these situations, a stronger solvent B may be required to increase the final elution power of the elution program. Of course, if the last band elutes well before the end of the elution program, separation time can be saved by terminating the elution program at the time of elution of the final sample band. On the other hand, if solvent A is too

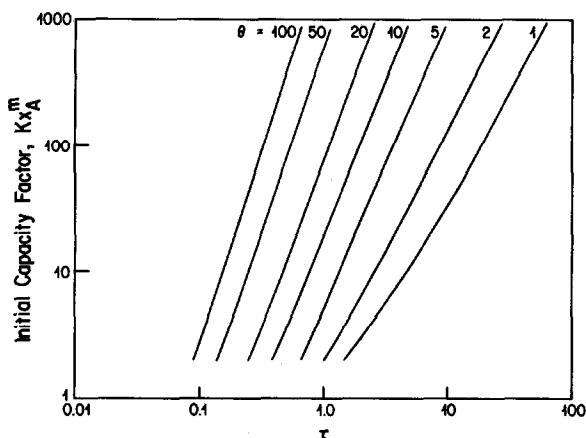


Fig. 3. Numerical results illustrating the effect of  $\theta$  at  $\kappa = 0.5$  and  $m = -2.5$ .

weak, the resolution of early eluting species may suffer. Consequently, solvents A and B must be properly chosen for the separation at hand.

Another parameter of importance in GFP is gradient steepness; *i.e.*, the rate of change of solvent composition with time. This is given by

$$\frac{dx}{d\tau} = x_A \frac{[\kappa(\theta - 1)]}{(1 + \kappa\tau)^2} \quad (17)$$

The importance of gradient steepness parallels that of the capacity factor in isocratic elution. Thus as the solvent strength is increased in isocratic elution with a concomitant decrease in the capacity factor, the resolution of a given pair of adjacent bands decreases while the sensitivity (*i.e.*, the peak height-to-width ratio) increases and analysis time decreases. Thus a compromise between adequate resolution and sensitivity exists for an intermediate solvent strength which yields  $k'$  values in the neighborhood of 2–5. As with isocratic elution, there exists a similar compromise among sensitivity, resolution, and analysis time that favors some intermediate gradient steepness. Thus, as gradient steepness increases, resolution of adjacent bands decreases while sensitivity increases and analysis time decreases.

The effect of  $\theta$  at constant  $\kappa$  and  $m$  is summarized in Fig. 3. Note that the case  $\theta = 1$  is simply isocratic flow programming. Thus, the effect of increased elution strength, as measured by  $\theta$ , is illustrated. As shown, by increasing  $\theta$ , the dimensionless retention time,  $\tau$ , decreases for a given initial capacity factor. This is expected since an increase in  $\theta$  increases the gradient steepness and hence higher concentrations of electrolyte enter the column at earlier times; this promotes the elution of the components. One can show that by increasing  $\kappa$ , the lines of  $\theta$  are shifted to lower values of  $\tau$ . Once again, higher concentrations of the eluting species reach the column at earlier times and hence, elution is promoted. Experimental results illustrating the effect of  $\theta$  on the separation of OV and BSA are shown in Figs. 4–6. Note that at  $\theta = 5$ , the peaks are rather broad and resemble those of isocratic elution. By increasing  $\theta$ , the gradient steepness increases leading to decreased retention volumes and sharper peaks. However, if  $\theta$  is increased too much, the gradient steepness becomes too large and



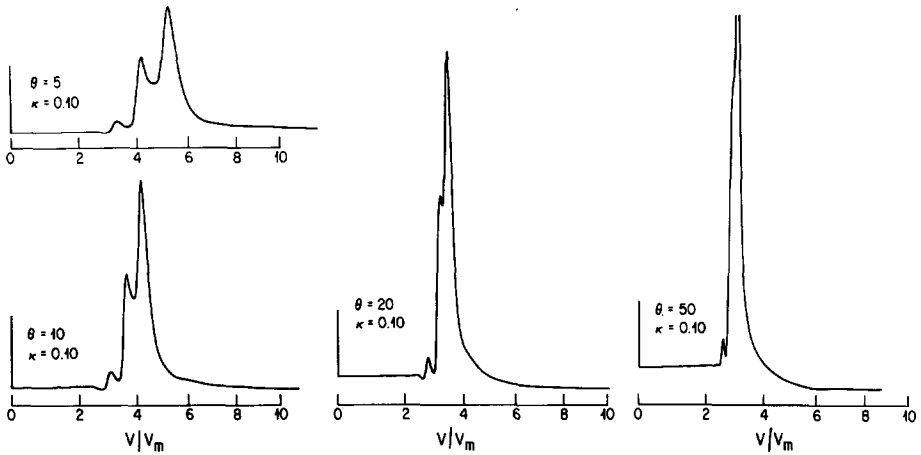


Fig. 4. Experimental results illustrating the effect of  $\theta$  at  $\kappa = 0.10$ .

resolution suffers. Consequently, the components can no longer be adequately resolved. Thus it can be seen that a decrease in gradient steepness leads to the following changes: (i) broader bands and decreased detection sensitivity; (ii) generally improved resolution; and (iii) increased separation volumes. Finally, note that the resolution of OV and BSA is adequate under most experimental conditions and is comparable or marginally better than that of normal gradient elution under typical operating conditions as illustrated in Fig. 7. However, as previously stated, one advantage of GFP is an increase in front-end resolution due to increased column efficiency for the early eluting components. This effect will be illustrated shortly.

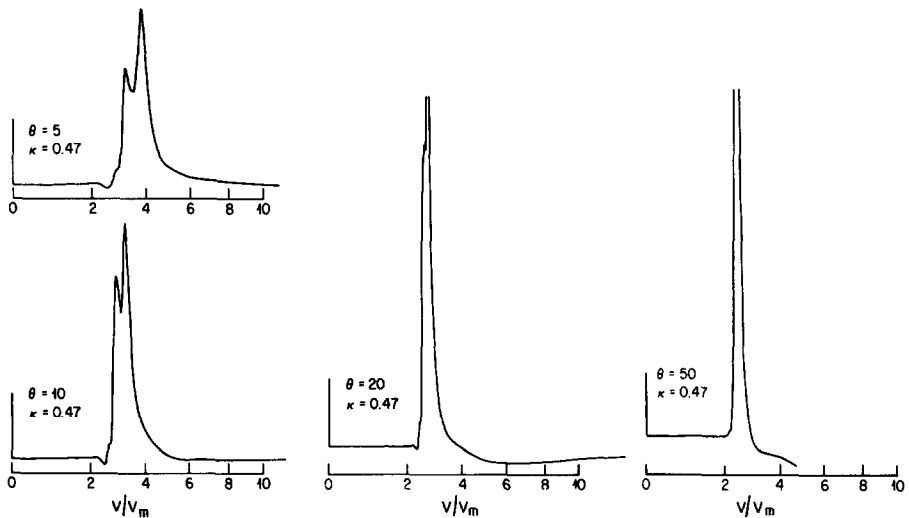


Fig. 5. Experimental results illustrating the effect of  $\theta$  at  $\kappa = 0.47$ .

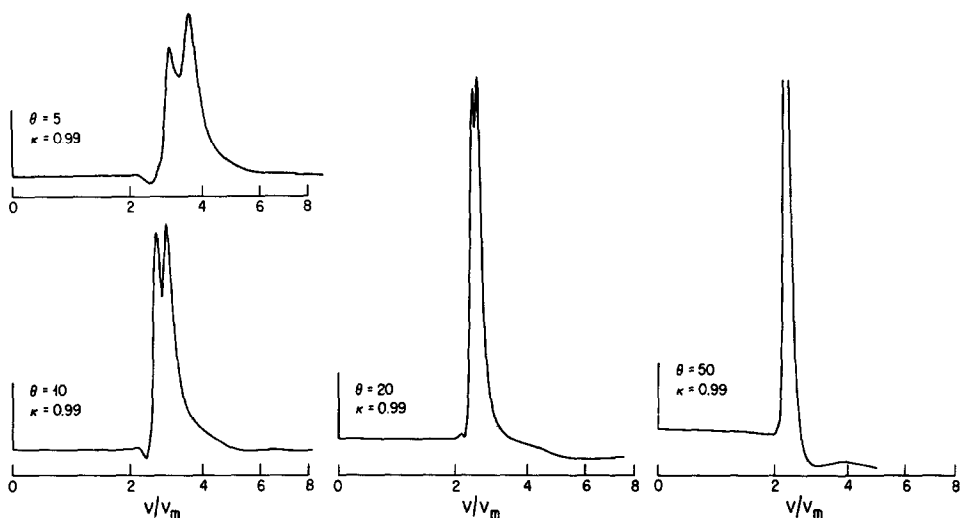


Fig. 6. Experimental results illustrating the effect of  $\theta$  at  $\kappa = 0.99$ .

*The effect of the relative increase in flow-rate as reflected through  $\kappa$*

The definition of  $\kappa$  is given by eqn. 14. Multiplication of eqns. 12 and 14 yields

$$\kappa\tau = \frac{bt}{a} \quad (18)$$

Thus  $\kappa$  gives an indication of the increase in the volumetric flow-rate as compared to the initial flow-rate. Note that for  $\kappa\tau = 1$ , pump A and pump B are delivering the same volumetric flow-rate. For  $\kappa\tau < 1$ , pump A delivers the bulk of the solvent to the column whereas for  $\kappa\tau > 1$ , pump B delivers the majority of the solvent to the column.

The effect of  $\kappa$  at constant  $m$  and  $\theta$  on  $\tau$  is summarized in Fig. 8. As illustrated, by increasing  $\kappa$ , the dimensionless retention time  $\tau$  decreases for a given initial capacity

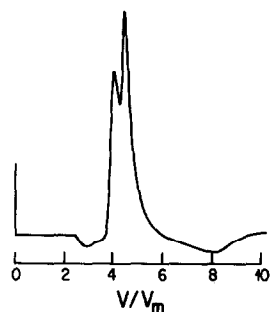


Fig. 7. Normal gradient elution of BSA and OV at pH 7.00. Elution was performed with a 30-min linear gradient from buffer alone to buffered 0.2 M ammonium sulfate.

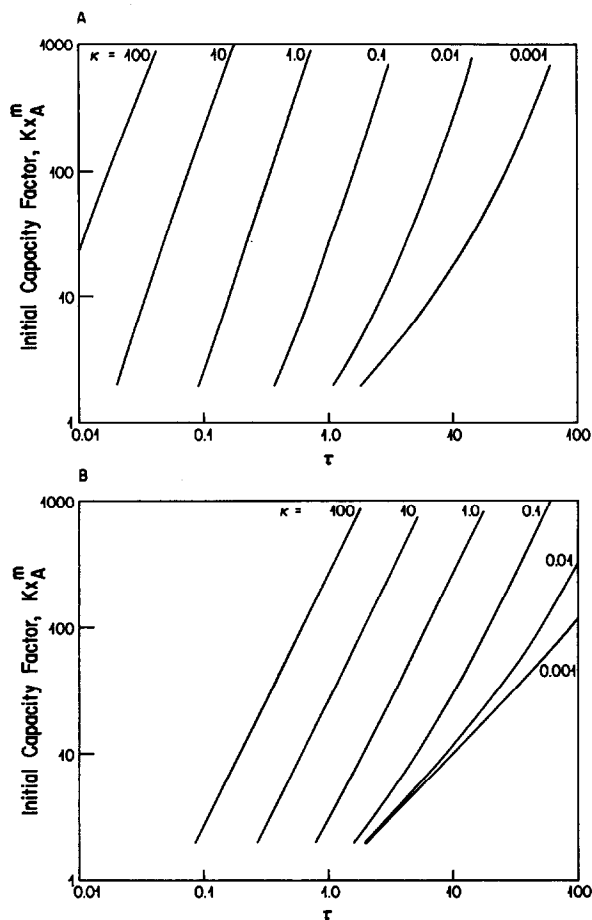


Fig. 8. Numerical results illustrating the effect of  $\kappa$  at (A)  $\theta = 50$  and (B)  $\theta = 2$ .  $m = -2.5$ .

factor. This would be expected even under isocratic conditions due to the increase in the flow-rate; however, the effect becomes accentuated as  $\theta$  increases due to an increase in the elution power of the mobile phase. Experimental results illustrating the effect of  $\kappa$  are shown in Figs. 9–11.

Once again, for low values of  $\theta$  and  $\kappa$ , the chromatograms resemble those of normal elution. By increasing either  $\theta$  or  $\kappa$ , elution is achieved by increasing the solvent strength and hence the migration of the components. Although the peaks become less broad, resolution also decreases.

As was previously stated, a driving force behind the development of GFP was in response to the poor resolution of early bands when the weakest possible solvent A is used. The proposed solution was to increase the plate number  $N$  by initially employing a low flow-rate. Thus, by increasing column efficiency, front-end resolution should be improved. This is illustrated in Fig. 12. In each case the final flow-rate is approximately the same. Consequently,  $\kappa = 0.10$  represents a higher initial flow-rate than  $\kappa = 0.47$  which in turn is higher than for  $\kappa = 0.99$ . Note that by decreasing the initial flow-rate,

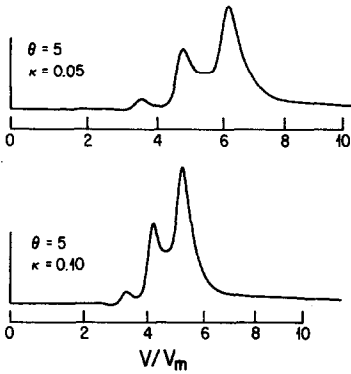


Fig. 9. Experimental results illustrating the effect of  $\kappa$  at  $\theta = 5$ .

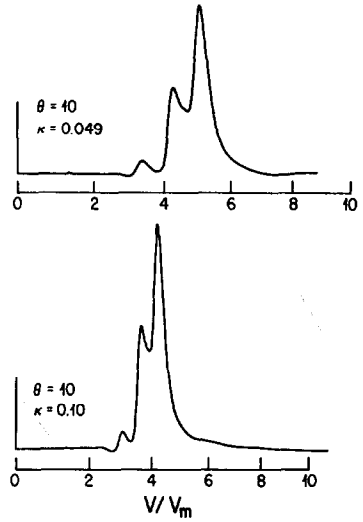


Fig. 10. Experimental results illustrating the effect of  $\kappa$  at  $\theta = 10$ .

an improvement in resolution occurs due to increased column efficiency even for components which have observed capacity factors in the desirable range of approximately 2–5. Greater enhancement of resolution is expected for bands which are poorly retained (i.e.  $k' < 2$ ).

#### Comparison between theory and experiment

Eqns. 5, 6 and 11 represent an idealized case for GFP in that they neglect the dwell volume of the apparatus. In many situations, this dwell volume  $V_D$  can be

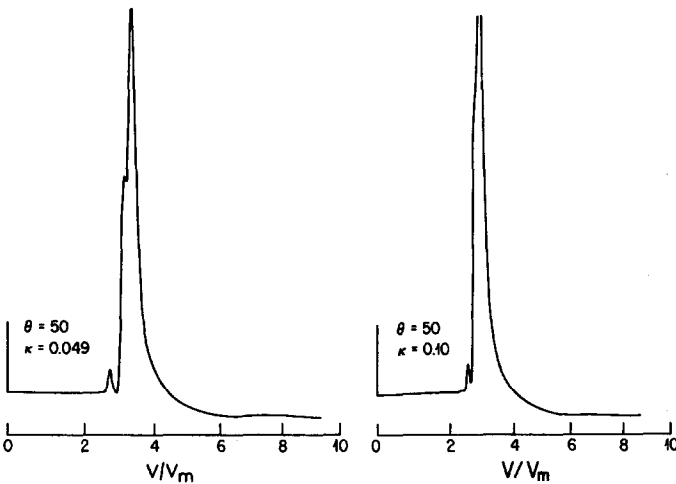


Fig. 11. Experimental results illustrating the effect of  $\kappa$  at  $\theta = 50$ .

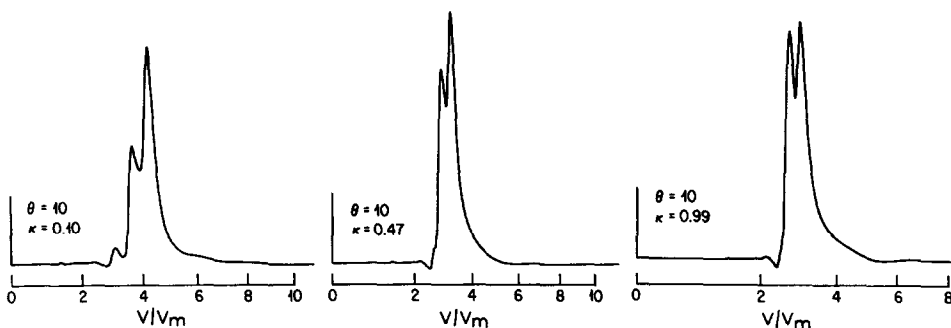


Fig. 12. Experimental results illustrating the improvement of resolution by decreasing the initial flow-rate.

significant and must be corrected for. To account for this non-ideality, the previous mathematical development is easily modified. The gradient composition now becomes

$$x = \frac{ax_A + b(t - t_D)x_B}{a + b(t - t_D)} \quad t > t_D \quad (19)$$

$$x = x_A \quad t \leq t_D \quad (20)$$

where  $t_D$  is the dwell time. The dwell time is simply the holdup time between the point where solvent mixing occurs and where the mixed solvent reaches the column inlet. Consequently, the fundamental equation for gradient elution becomes

$$\int_0^{\tau_D} (1 + \kappa\tau) d\tau + \int_{\tau_D}^{\tau} \frac{(1 + \kappa\tau)[1 + \kappa(\tau - \tau_D)]^m}{[1 + \kappa\theta(\tau - \tau_D)]^m} = Kx_A^m \quad (21)$$

where  $\tau_D$  is the dimensionless dwell time. The first integral on the left-hand side of eqn. 21 is solved analytically whereas the second integral is solved numerically. These two integrals are then added and checked against the right-hand side of eqn. 21, which can be calculated from the parameters of Table I and then compared to the observed results. Table II summarizes the comparison between calculations employing eqn. 21 and the experimental results. The agreement is acceptable if one realizes the numerous sources of error involved. For example, the isocratic retention parameters (see Fig. 2) do not precisely fit the data. Thus, when the left-hand side of eqn. 21 is integrated numerically and checked against the calculated initial capacity factor (*i.e.*  $Kx_A^m$ ), a large error in  $\tau_g$  can occur due to the range of initial capacity factors (*i.e.*,  $Kx_A^m$ ) which are within the confidence interval predicted by eqn. 7.

## CONCLUSIONS

GFP provides a new method of attack on the general elution problem by combining the desirable features of gradient elution and flow programming. The method may prove useful when front-end resolution is poor and the weakest possible chromatographic solvent is already being employed. Experimental results with two

TABLE II

COMPARISON BETWEEN EXPERIMENTAL AND THEORETICAL RESULTS IN GFP

$\theta$		Observed retention time (min)	$\tau_D$	$\tau_R$	Calculated retention time (min)
$\kappa = 0.049 \pm 0.006$ ; $\tau_D = 1.0$ ; $\tau_m = 0.98$ ; $V_m/a = 4.63$ min					
$5.00 \pm 0.33$	BSA	19.8	4.43	5.41	25.0
	OV	25.3	5.14	6.12	28.3
$10.0 \pm 0.6$	BSA	18.0	3.35	4.33	20.0
	OV	21.0	3.72	4.70	21.8
$20.0 \pm 1.2$	BSA	15.5	2.57	3.55	16.4
	OV	17.0	2.76	3.74	17.3
$50.0 \pm 3.5$	BSA	13.0	1.89	2.87	13.2
	OV	14.3	1.97	2.95	13.7
$\kappa = 0.47 \pm 0.04$ ; $\tau_D = 0.86$ ; $\tau_m = 0.84$ ; $V_m/a = 6.65$ min					
$5.00 \pm 0.33$	BSA	14.3	1.85	2.69	17.8
	OV	16.3	1.98	2.82	18.7
$10.0 \pm 0.6$	BSA	13.0	1.46	2.30	15.2
	OV	14.0	1.51	2.35	15.6
$20.0 \pm 1.2$	BSA	11.8	1.22	2.06	13.7
	OV	12.3	1.25	2.09	13.9
$50.0 \pm 3.5$	BSA	11.3	1.05	1.89	12.6
	OV	11.3	1.06	1.90	12.6
$\kappa = 0.99 \pm 0.15$ ; $\tau_D = 0.75$ ; $\tau_m = 0.73$ ; $V_m/a = 11.9$ min					
$5.00 \pm 0.33$	BSA	19.5	1.36	2.09	24.8
	OV	22.3	1.44	2.17	25.8
$10.0 \pm 0.6$	BSA	18.0	1.10	1.83	21.7
	OV	19.3	1.13	1.86	22.1
$20.0 \pm 1.2$	BSA	16.8	0.96	1.69	20.1
	OV	17.3	0.97	1.70	20.2
$50.0 \pm 3.5$	BSA	16.3	0.86	1.59	18.9
	OV	16.3	0.86	1.59	18.9

model proteins and an anion-exchange column illustrate the method as a function of various characteristic parameters. Resolution is good and results compare favorably to theory in view of the experimental errors involved. Improved resolution due to increased column efficiency is also demonstrated.

## REFERENCES

- 1 L. R. Snyder, *J. Chromatogr. Sci.*, 8 (1970) 692.
- 2 L. R. Snyder and J. J. Kirkland, *Introduction to Modern Liquid Chromatography*, Wiley, New York, 1974, p. 38.
- 3 L. R. Snyder, in Cs. Horváth (Editor), *High Performance Liquid Chromatography — Advances and Perspectives*, Vol. 1, Academic Press, New York, 1980.
- 4 P. A. Jandera and J. Churacek, *Adv. Chromatogr. (N.Y.)*, 19 (1981) 125.
- 5 N. K. Boardman and S. M. Partridge, *Biochem. J.*, 59 (1955) 543.
- 6 W. Kopaciewicz, M. A. Rounds, J. Fausnaugh and F. F. Regnier, *J. Chromatogr.*, 266 (1983) 3.